MOLECULAR AND CELLULAR BIOLOGY, Aug. 1996, p. 4478–4485 Vol. 16, No. 8
0270-7306/96/$04.00+0

Loss of Sustained Fus3p Kinase Activity and the G_1 Arrest Response in Cells Expressing an Inappropriate Pheromone Receptor

ANDRÉS COUVE AND JEANNE P. HIRSCH*

Department of Cell Biology and Anatomy, Mount Sinai School of Medicine, New York, New York 10029

Received 27 February 1996/Returned for modification 12 April 1996/Accepted 23 May 1996

The yeast pheromone response pathway is mediated by two G protein-linked receptors, each of which is expressed only in its specific cell type. The *STE3^{DAF}* mutation results in inappropriate expression of the a-factor receptor in *MAT*a cells. Expression of this receptor in the inappropriate cell type confers resistance to pheromone-induced G_1 arrest, a phenomenon that we have termed receptor inhibition. The ability of *STE3^{DAF}* cells to cycle in the presence of pheromone was found to correlate with reduced phosphorylation of the cyclin-dependent kinase inhibitor Far1p. Measurement of Fus3p mitogen-activated protein (MAP) kinase activity in wild-type and *STE3^{DAF}* cells showed that induction of Fus3p activity was the same in both strains at times of up to 1 h after pheromone treatment. However, after 2 or more hours, Fus3p activity declined in *STE3^{DAF}* cells but remained high in wild-type cells. The level of inducible *FUS1* RNA paralleled the changes seen in Fus3p activity. Short-term activation of the Fus3p MAP kinase is therefore sufficient for the early transcriptional induction response to pheromone, but sustained activation is required for cell cycle arrest. Escape from the cell cycle arrest response was not seen in wild-type cells treated with low doses of pheromone, indicating that receptor inhibition is not simply a result of weak signaling but rather acts selectively at late times during the response. *STE3^{DAF}* was found to inhibit the pheromone response pathway at a step between the G_β subunit and Ste5p, the scaffolding protein that binds the components of the MAP kinase phosphorylation cascade. Overexpression of Ste20p, a kinase thought to act between the G protein and the MAP kinase cascade, suppressed the *STE3^{DAF}* phenotype. These findings are consistent with a model in which receptor inhibition acts by blocking the signaling pathway downstream of G protein dissociation and upstream of MAP kinase cascade activation, at a step that could directly involve Ste20p.

Extracellular signals often impinge on cells through a central pathway that acts on different substrates to generate the cellular responses. In the yeast *Saccharomyces cerevisiae*, the responses to extracellular pheromone include cell cycle arrest, transcriptional induction and repression, and morphological changes that result in projection formation (reviewed in reference 49). These responses all depend on a signaling pathway that is activated by binding of pheromone to a G protein-linked receptor, which causes dissociation of its associated heterotrimeric G protein and activation of a mitogen-activated protein (MAP) kinase cascade (16). The targets of this signaling pathway that carry out the specific responses include Ste12p, a transcription factor that mediates the induction of pheromone-inducible genes (14, 53), and Far1p, a cyclin-dependent kinase inhibitor that mediates cell cycle arrest (2, 40, 41). Little is known about potential differences in the requirements of individual target proteins for the central signal.

Yeast cells that contain the *MAT***a** allele normally express the α-factor receptor, Ste2p, and secrete **a**-factor, encoded by the *MFA1* and *MFA2* genes. We have recently described a phenomenon in which *MAT***a** cells that inappropriately express the **a**-factor receptor display resistance to pheromone-induced cell cycle arrest. This process, termed receptor inhibition, was originally uncovered by a screen for dominant mutations that eliminated pheromone-induced arrest in *MAT***a** cells (7). The *DAF2* mutation (called *DAF* for dominant alpha-factor resistance) is an allele of *STE3*, the **a**-factor receptor gene, that results in its inappropriate expression in *MAT***a** cells (26). The *STE3^{DAF}* allele has a rearranged 5′ flanking region containing a repetitive element that causes it to be expressed in all cell types. The level of *STE3* RNA transcribed from the inserted promoter is similar to the normal level of this RNA in α cells, so the *DAF* phenotype is not the result of overexpression of the receptor. We have been characterizing the process of receptor inhibition to provide information about this novel receptor function and to yield insights about normal signaling processes.

The two classes of proteins known to interact with G protein-linked receptors are G_α subunits and kinases involved in desensitization (31). Our genetic results indicate that the Ste3p pheromone receptor can interact, either directly or indirectly, with components of the signaling pathway other than G_α. This conclusion comes from the observation that *STE3^{DAF}* blocks the constitutive cell cycle arrest phenotype caused by deletion of the *GPA1* gene, which encodes the G_α subunit (7, 26). Therefore, *STE3^{DAF}* does not exert its effect by uncoupling the Ste2p receptor from its associated G_α subunit, as occurs during desensitization of mammalian G protein-linked receptors (22). In fact, *STE3^{DAF}* is capable of inhibiting the constitutive cell cycle arrest phenotype of a Δ*gpa1* strain that contains a deletion of the *STE2* gene, indicating that the α-factor receptor is not involved in this process. These findings demonstrate that receptor inhibition by *STE3^{DAF}* must act downstream of the G_α subunit to decrease the amount or type of signal generated by another component of the pathway.

In the study described here, we show that *STE3^{DAF}* causes a late inhibition of the signaling pathway that results in a nearly complete block cell of cycle arrest. These effects correlate with the fact that Fus3p MAP kinase activity increases at the same rate in both wild-type and *STE3^{DAF}* cells for about 1 h of

* Corresponding author. Phone: (212) 241-0224. Fax: (212) 860-1174.

TABLE 1. Strains used[a]

Strain	Genotype	Source
W303	*MAT***a**/**α** *leu2-3,112 trp1-1 can1-100 ura3-1 ade2-1 his3-11,15*	R. Rothstein
W3031A	*MAT***a** *leu2-3,112 trp1-1 can1-100 ura3-1 ade2-1 his3-11,15*	R. Rothstein
H63-19C	*MAT***a** *TRP1*::*STE3*$^{DAF2.5}$	This study
H63-14C	*MAT***a** *mfa1-Δ3*::*HIS3 mfa2-Δ2*::*HIS3*	This study
H63-8A	*MAT***a** *mfa1-Δ3*::*HIS3 mfa2-Δ2*::*HIS3 TRP1*::*STE3*$^{DAF2.5}$	This study
H67-9D.Ba	*MAT***a** *mfa1-Δ3*::*HIS3 mfa2-Δ2*::*HIS3 sst1*::*hisG*	This study
H67-6C.Ba	*MAT***a** *mfa1-Δ3*::*HIS3 mfa2-Δ2*::*HIS3 STE3*$^{DAF2.5}$ *sst1*::*hisG*	This study
H67-9D.FBa	*MAT***a** *mfa1-Δ3*::*HIS3 mfa2-Δ2*::*HIS3 LEU2*::*GAL1*::*FAR1*/+*N sst1*::*hisG*	This study
H67-6C.FBa	*MAT***a** *mfa1-Δ3*::*HIS3 mfa2-Δ2*::*HIS3 STE3*$^{DAF2.5}$ *LEU2*::*GAL1*::*FAR1*/+*N sst1*::*hisG*	This study
AC9-F1	*MAT***a** *mfa1-Δ3*::*HIS3 mfa2-Δ2*::*HIS3 sst1*::*hisG cln1*::*LEU2 far1*::*URA3*	This study
AC8-F1	*MAT***a** *mfa1-Δ3*::*HIS3 mfa2-Δ2*::*HIS3 STE3*$^{DAF2.5}$ *sst1*::*hisG cln1*::*LEU2 far1*::*URA3*	This study
AC3-F1	*MAT***a** *mfa1-Δ3*::*HIS3 mfa2-Δ2*::*HIS3 sst1*::*hisG cln2*::*LEU2 far1*::*URA3*	This study
AC2-F1	*MAT***a** *mfa1-Δ3*::*HIS3 mfa2-Δ2*::*HIS3 STE3*$^{DAF2.5}$ *sst1*::*hisG cln2*::*LEU2 far1*::*URA3*	This study
AC5-F1	*MAT***a** *mfa1-Δ3*::*HIS3 mfa2-Δ2*::*HIS3 sst1*::*hisG cln3*::*LEU2 far1*::*URA3*	This study
AC4-F1	*MAT***a** *mfa1-Δ3*::*HIS3 mfa2-Δ2*::*HIS3 STE3*$^{DAF2.5}$ *sst1*::*hisG cln3*::*LEU2 far1*::*URA3*	This study
AC12	*MAT***a** *mfa1-Δ3*::*HIS3 mfa2-Δ2*::*HIS3 sst1*::*hisG far1*::*URA3*	This study
D109-1B	*MAT***a** *ste12*::*LEU2*	This study

[a] All of the strains other than W303 and W3031A are isogenic to W3031A.

pheromone treatment, after which Fus3p activity remains high in wild-type cells but declines in *STE3*^{DAF} cells. Genetic analysis showed that the late decrease in activity conferred by the receptor acts on the pathway at a step after G protein dissociation but at or before the Ste5p step.

MATERIALS AND METHODS

Plasmid construction. Null alleles of the *MFA1* and *MFA2* genes disrupted with *HIS3* were constructed from existing *LEU2* and *URA3* disruption alleles (37) as follows. For the *MFA1* disruption, the *HIS3* gene on a 1.7-kb *Sal*I-*Sma*I fragment from pUC18::HIS3 was cloned into the *Xho*I-*Hpa*I sites of pSM86 to create pmfa1-Δ3::HIS3. For the *MFA2* disruption, pSM35 was digested with *Sma*I and *Eco*RV and religated to remove the *URA3* gene, and then the *HIS3* gene on a 1.7-kb *Bam*HI fragment from pUC18::HIS3 was cloned into the *Bam*HI site of pSM35 to create pmfa2-Δ2::HIS3. To construct a *URA3* version of pGA1903, which contains a myc-tagged *FUS3* gene under control of the *TPI1* promoter (55), a 1.2-kb *Xba*I fragment containing the *URA3* gene from pAC100-2 was cloned into the *Xba*I site in the *TRP1* gene of pGA1903 to produce pGA1903-U. To construct a *URA3* disruption of *FAR1*, a 1.2-kb *Hin*dIII-*Bam*HI fragment from pAC100-2 was cloned into the *Hin*dIII-*Bam*HI sites of *FAR1* in pJM306 (36) to produce pfar1-U1. To construct a *LEU2* disruption of *CLN1*, a 2.9-kb *Bgl*II fragment from YEp13 was cloned into the *Bgl*II sites in the *HIS3* portion of the *cln1*::*HIS3* gene in pMT256 (51) to produce pcln1-L2. To construct a plasmid containing the *STE5*^{Hyp} allele (21) under the control of the *GAL* promoter, a 3.2-kb *Pst*I-*Dra*I fragment from pDJ174 (kindly provided by D. Jenness) containing the *STE5*^{Hyp} gene was first cloned into the *Pst*I-*Sma*I sites of Bluescript, and then the 3.2-kb *Bam*HI fragment from this construct was cloned into the *Bam*HI site of pBM272 to create pGAL-STE5H. To construct a *LEU2* plasmid containing the *GAL-STE20* gene, a fragment creating a myc-tagged *STE20* was generated by PCR (9) with oligonucleotide primers oSTE20-1 (5′-CCTCTAGAAATGGAGCAAAAGCTCATTTCTGAA GAGGACTTGAATAGCAATGATCCATCT-3′) and oSTE20-2 (5′ACTGCTT CTAGAGATTTG-3′). The template used for PCR was plasmid pDH166, which contains the entire coding region of *STE20* under the control of the *GAL* promoter (kindly provided by M. Whiteway). The *Spe*I-*Xba*I N-terminal fragment of pDH166 was then replaced with the myc-tagged *STE20* PCR fragment digested with *Xba*I to produce pMSTE20. The *Xho*I-*Sac*II fragment from pMSTE20 was subcloned into the *Xho*I-*Sac*II sites of pRS315 (47) to create pMSTE20-L2.

Strains and media. Strains used in this study are listed in Table 1. *STE3*^{DAF} alleles were made from the integrating plasmid piDAF2m-5, which contains the *STE3*$^{DAF2-2}$ gene (26). The *TRP1*::*STE3*$^{DAF2.5}$ allele was made by linearizing piDAF2m-5 with *Xba*I to direct integration into *TRP1*; *STE3*$^{DAF2.5}$ was made by linearizing piDAF2m-5 with *Sal*I to direct integration into *STE3*. Disruptions of the **a**-factor genes were made by transformation with a 3.8-kb *Eco*RI-*Xba*I fragment from pmfa1-Δ3::HIS3 to create *mfa1-Δ3*::*HIS3* and by transformation with a 3.2-kb *Eco*RI fragment from pmfa2-Δ2::HIS3 to create *mfa2-Δ*::*HIS3*. The *sst1*::*hisG* allele was constructed by transformation with a 5.7-kb *Eco*RI-*Sal*I fragment from pJGSST1 to create *sst1*::*URA3* followed by deletion of *URA3* from the chromosome through recombination of the adjacent *hisG* sequences as described previously (13). The *LEU2*::*GAL1*::*FAR1*/+*N* allele was made by linearizing pJM306 with *Cla*I to direct integration into *LEU2* (36). The *FAR1* gene was disrupted by transformation with an approximately 4-kb *Xho*I-*Sac*I fragment from pfar1-U1 to create *far1*::*URA3*. The *CLN*::*LEU2* disruptions were made with the following fragments: an approximately 5-kb *Pvu*II fragment from pcln1-L2 for *cln1*::*LEU2*, a 3.5-kb *Pvu*II fragment from pMT160 (51) for *cln2*::*LEU2*, and a 3-kb *Sac*I fragment from pBFcln3Δ::leu for *cln3*::*LEU2*. All strain constructions involving transformations were confirmed by Southern blot.

Strains were grown on YEPD (2% glucose) or YEP-Gal (3% galactose), and strains under selection were grown on synthetic dropout media, as described previously (46).

Yeast methods. Yeast transformations were performed by the lithium acetate method (27) modified as described previously (26). Yeast RNA was extracted from cells as described previously (8).

Preparation of cell extracts for immunoprecipitation was done by modification of a method described previously (15). Samples (20 ml) of log-phase cells were pelleted, resuspended in 1.25 ml of stop buffer (50 mM Tris-HCl [pH 7.5], 150 mM NaCl, 5 mM EDTA, 0.1% Nonidet P-40 [NP-40], 15 mM *p*-nitrophenyl phosphate [NPP], 15 mM $Na_2H_2P_2O_7$, 10 mM NaF, 0.1 mM sodium orthovanadate [Na_3VO_4], 5 mM phenylmethylsulfonyl fluoride [PMSF]), and pelleted again. The cells were resuspended in lysis buffer (stop buffer plus 25 mM HEPES [*N*-2-hydroxyethylpiperazine-*N*′-2-ethanesulfonic acid] [pH 7.2] with 40 μg of aprotinin per ml and 20 μg of leupeptin per ml), and approximately 0.25 ml of glass beads was added to the tube. The suspension was vortexed 8 to 10 min and centrifuged for 5 min at 4°C. After estimating the volume of the lysates, 2/3 volume of a saturated ammonium sulfate solution was added and the samples were incubated on a rocker for 30 min at 4°C. The precipitates were pelleted in a microcentrifuge for 10 min and resuspended in storage buffer (25 mM HEPES [pH 8.0]), 5 mM EDTA, 150 mM NaCl, 0.1% NP-40, 20% glycerol, 15 mM NPP, 0.1 mM Na_3VO_4, 1 mM PMSF, 40 μg of aprotinin per ml, 20 μg of leupeptin per ml). The protein concentration of the samples was determined by a bicinchoninic acid protein assay kit (Pierce), and the samples were aliquoted, flash frozen in liquid nitrogen, and stored at −80°C.

Cell extracts used for Far1p immunoblots were prepared by growing cells in YEP-Gal overnight to induce expression of Far1p. The washed log-phase cells were resuspended in 200 μl of lysis buffer (50 mM Tris-HCl [pH 8.0], 1% sodium dodecyl sulfate [SDS], 1 mM PMSF, and 1 μg each of leupeptin, aprotinin, chymostatin, and pepstatin per ml) and frozen in a dry ice/ethanol bath. After thawing, the cell suspension was lysed with approximately 0.25 ml of glass beads by vortexing for 10 min at 4°C and centrifuging for 5 min at 4°C to clear the lysate. The protein concentration was determined, and equal amounts of protein (40 μg) were loaded in each lane for SDS-polyacrylamide gel electrophoresis (SDS-PAGE). For experiments performed with the anti-myc antibody, in which both immunoprecipitation and immunoblotting were done on the same samples, the extracts were prepared by the immunoprecipitation method.

Halo assays were performed by plating a lawn of cells to be tested, placing a filter paper disk containing 5 μl of 1 mM α-factor onto the plate, and incubating it at 30°C for 2 days.

Northern (RNA) blots. RNA was transferred to a nitrocellulose membrane after formaldehyde-agarose gel electrophoresis as described previously (32). The membranes were UV cross-linked by using a Stratalinker UV box. Prehybridization and hybridization were done at 65°C in a buffer containing 1 M NaCl, 10 mM Tris-HCl (pH 7.5), 1 mM EDTA, and 5% SDS. The probes used were gel-purified DNA restriction fragments ^{32}P labeled by random primer labeling with a Prime-It kit (Stratagene). The fragments used were *FUS1*, a 1.4-kb

*Eco*RI-*Hin*dIII fragment from plasmid pSL589 (35), and *TCM1* (45), a 0.8-kb *Hpa*I-*Sal*I fragment from plasmid pAB309Δ.

Immunoblots and immune-complex kinase assays. For immunoblots to detect Far1p, SDS-PAGE was performed with a 6% polyacrylamide gel, separated proteins were transferred to nitrocellulose, and the blot was probed with an anti-Far1p (51-830) rabbit polyclonal antibody (36) at a 1/5,000 dilution. Donkey anti-rabbit immunoglobulin horseradish peroxidase (Amersham) was used at a dilution of 1/7,500, and immune complexes were detected with an enhanced chemiluminescence kit (Amersham).

Proteins were immunoprecipitated from cell extracts by incubating 100 μg of protein with 1.7 μg of Myc1-9E10 antibody (Oncogene Science) (17) on a rocker for 60 min at 4°C. Protein A-Sepharose beads were swelled in 0.1 M Tris-HCl (pH 7.5) for 15 min at room temperature, washed two times in 0.1 M Tris-HCl (pH 7.5), washed three times in kinase extract buffer (50 mM Tris-HCl [pH 7.5], 150 mM NaCl, 5 mM EDTA, 0.1% NP-40), and resuspended in an equal volume of kinase extract buffer plus 5 mg of bovine serum albumin per ml, 15 mM NPP, 0.1 mM Na_3VO_4, 1 mM PMSF, 40 μg of aprotinin per ml, and 20 μg of leupeptin per ml. The beads were incubated on a rocker for 60 min at 4°C, and 25 μl of equilibrated beads in 0.5 ml of kinase extract buffer plus 5 mg of bovine serum albumin per ml, 15 mM NPP, 0.1 mM Na_3VO_4, 1 mM PMSF, 40 μg of aprotinin per ml, and 20 μg of leupeptin per ml were added to the antigen-antibody complexes. These mixtures were incubated on a rocker for 90 min at 4°C. The immune complexes were washed five times with buffer A (50 mM Tris-HCl [pH 7.5], 150 mM NaCl, 5 mM EDTA, 0.1% NP-40, 15 mM NPP, 0.1 mM Na_3VO_4), three times with buffer B (25 mM HEPES, 15 mM NPP, 0.1 mM Na_3VO_4), and one time with buffer C (wash B with 15 mM $MgCl_2$). Kinase assays were performed with by adding 10 μl of 2× kinase assay buffer (50 mM HEPES [pH 7.5], 30 mM $MgCl_2$, 10 mM EGTA [ethyleneglycol-bis(β-aminoethylether)-*N*,*N*,*N*′,*N*′-tetraacetic acid], 2 mM dithiothreitol, 30 mM NPP, 0.2 mM Na_3VO_4, 80 μg of aprotinin per ml, 40 μg of leupeptin per ml), 7.5 μl of myelin basic protein (1 μg/μl), and 2.2 μl of ATP mix (2 μl of 1 mM ATP and 0.2 μl of [γ-^{32}P]ATP [10 μCi/μl]) to the adsorbed immune complexes. The reaction mixtures were incubated for 20 min at 30°C, and the reactions were stopped by the addition of 15 μl of 2× SDS-PAGE loading buffer. Before loading on a gel, the samples were incubated for 5 min at 100°C and 3 μl of 1 mM ATP was added to them. The beads were then pelleted, and 30 μl of supernatant was loaded. Before drying, the gels were fixed in 10% methanol, 10% acetic acid, 0.5% phosphoric acid, and 10 mM KH_2PO_4 for 1 h and then in 10% methanol and 10% acetic acid for 30 min.

RESULTS

*MAT***a** cells that carry the *STE3*^{DAF} allele are defective for pheromone-induced cell cycle arrest. To characterize the requirements for this phenotype, the effect of the *STE3*^{DAF} allele was investigated in strains containing mutations in other genes involved in the pheromone response.

Requirements for a-factor production and *FAR1* function. *MAT***a** *STE3*^{DAF} cells express both **a**-factor and the **a**-factor receptor and thus can bind the ligand that they secrete, potentially leading to continuous activation of the pheromone response pathway. The phenotype of *STE3*^{DAF} cells was therefore tested in strains with functional or nonfunctional copies of the *MFA1* and *MFA2* genes to assess the requirement for **a**-factor production. The degree of cell cycle arrest in these strains was determined by halo assays (Fig. 1A). *STE3*^{DAF} blocked cell cycle arrest in *mfa1 mfa2* strains as well as it did in *MFA1 MFA2* strains, demonstrating that inhibition of arrest is not the result of desensitization due to autocrine signaling. All subsequent experiments were therefore performed in *mfa1 mfa2* strains to eliminate any effects from the occupied Ste3p receptor.

The cell cycle inhibitor Far1p mediates arrest in response to pheromone by binding to Cdc28p-Cln1p and Cdc28p-Cln2p complexes and inhibiting their kinase activity (40, 41, 51). Although Far1p plays a major role in arresting the cell cycle, a Far1p-independent arrest mechanism is also thought to exist. This other mechanism is not apparent in wild-type cells but can be seen in a strain lacking both Far1p and Cln2p, which arrests at high doses of pheromone (2, 51). The *FAR1* gene was disrupted in the *STE3* and *STE3*^{DAF} strains containing Δ*cln* alleles to determine the effect of *STE3*^{DAF} on Far1p-independent cell cycle arrest. As expected, the Δ*cln2* Δ*far1* strain arrested in response to pheromone. However, the Δ*cln2* Δ*far1*

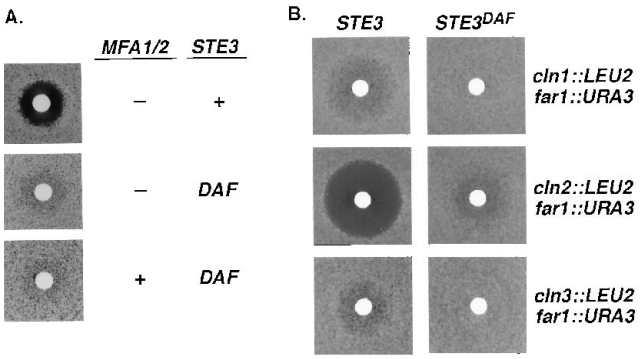

FIG. 1. Inhibition of G_1 arrest by *STE3*^{DAF} in *MAT***a** cells is independent of **a**-factor production and acts on Far1p-dependent and -independent mechanisms. (A) Halo assays were performed with 5 μl of 1 mM α-factor. The strains used were H63-14C, *MAT***a** *mfa1*::*HIS3 mfa2*::*HIS3* (top); H63-8A, *MAT***a** *mfa1*::*HIS3 mfa2*::*HIS3 STE3*^{DAF} (middle); and H63-19C, *MAT***a** *STE3*^{DAF} (bottom). (B) Halo assays were performed as for panel A. The strains used were AC9-F1, *MAT***a** *cln1*::*LEU2 far1*::*URA3*; AC8-F1, *MAT***a** *cln1*::*LEU2 far1*::*URA3 STE3*^{DAF}; AC3-F1, *MAT***a** *cln2*::*LEU2 far1*::*URA3*; AC2-F1, *MAT***a** *cln2*::*LEU2 far1*::*URA3 STE3*^{DAF}; AC5-F1, *MAT***a** *cln3*::*LEU2 far1*::*URA3*; and AC4-F1, *MAT***a** *cln3*::*LEU2 far1*::*URA3 STE3*^{DAF}.

STE3^{DAF} strain did not arrest (Fig. 1B), demonstrating that *STE3*^{DAF} also inhibits Far1p-independent arrest. Δ*far1* strains containing deletions of *CLN1* or *CLN3* also exhibited a significant decrease in pheromone sensitivity in a *STE3*^{DAF} background over that displayed in a *STE3* background, demonstrating that the small degree of Far1p-independent arrest displayed by these strains is subject to inhibition by *STE3*^{DAF}.

Receptor inhibition blocks cell cycle arrest by reducing Far1p phosphorylation. Far1p becomes phosphorylated on multiple sites during the pheromone response (3). Fus3p kinase and the Cdc28p-Cln complexes carry out some of these phosphorylations, which are thought to regulate Far1p activity (15, 40, 51). A time course experiment was performed to determine the state of Far1p in *STE3* and *STE3*^{DAF} strains during the response to pheromone. Far1p was detected by probing an immunoblot containing extracts from cells treated with α-factor for various amounts of time with an anti-Far1p antibody. Wild-type cells contained a significant amount of the slowest mobility form of Far1p at 15 min of α-factor treatment, and this form persisted throughout the time course up to 120 min (Fig. 2, lanes 7 to 10). *STE3*^{DAF} cells also contained the slowest mobility form of Far1p at 15 and 30 min of α-factor treatment (Fig. 2, lanes 2 and 3). However, at 60 and 120 min the level of fully phosphorylated Far1p was greatly decreased (Fig. 2, lanes 4 and 5). Therefore, the inhibitory effect of the *STE3*^{DAF} allele on cell cycle arrest correlates with the failure to maintain full phosphorylation of Far1p. This effect could be direct, or it

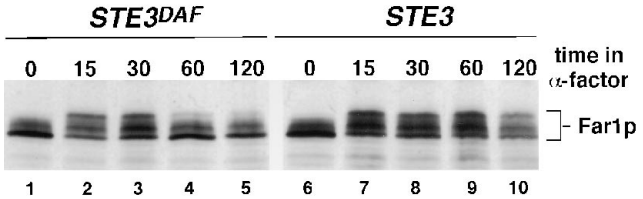

FIG. 2. Far1p is underphosphorylated in *STE3*^{DAF} cells. Log-phase cultures of *STE3*^{DAF} (H67-6C.FBa, lanes 1 to 5) and *STE3* (H67-9D.FBa, lanes 6 to 10) strains were treated with α-factor at 0.1 μM, and samples were removed at the times (in minutes) indicated. A Western blot was prepared from the samples and probed with anti-Far1p antibody.

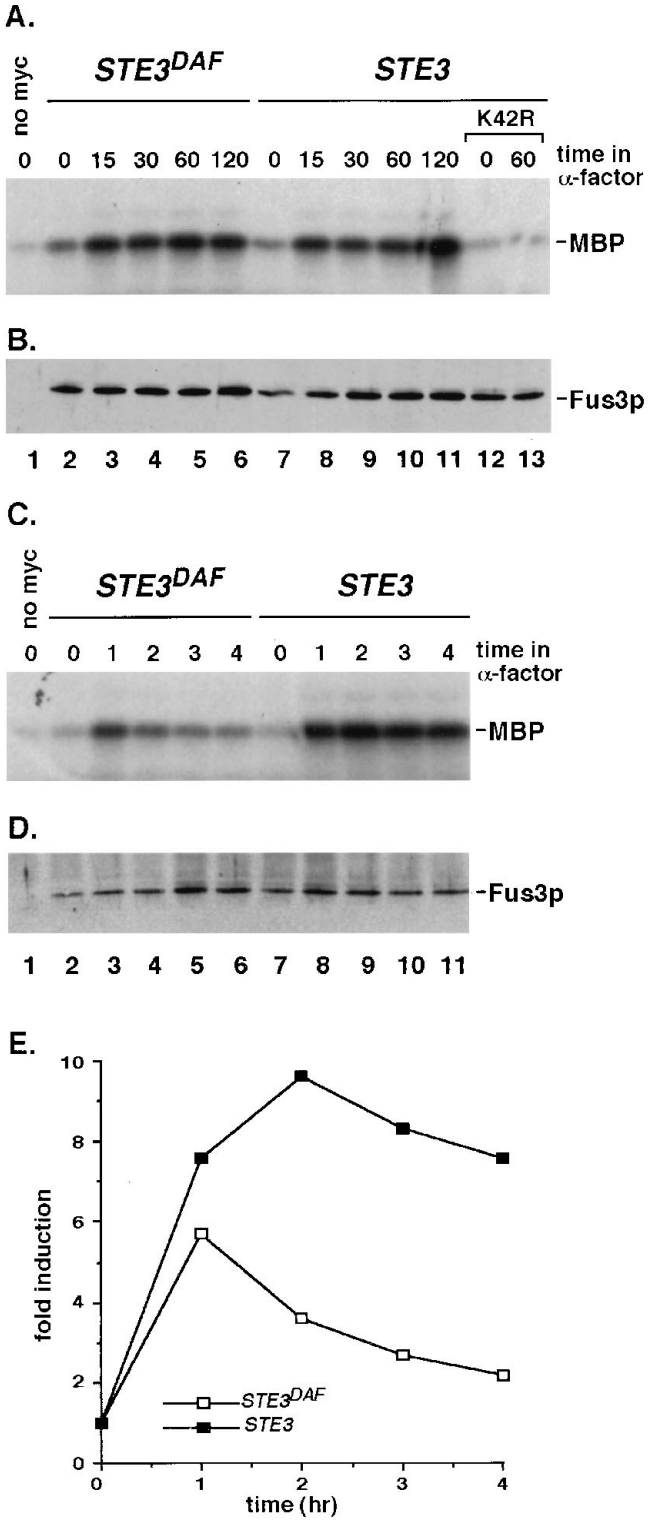

FIG. 3. Fus3p kinase activity is decreased at late times after pheromone treatment of *STE3*^{DAF} cells. (A) Log-phase cultures of a *STE3*^{DAF} strain (H67-6C.Ba) transformed with plasmid pGA1903-U (lanes 2 to 6) and a *STE3* strain (H67-9D.Ba) that was not transformed (lane 1) or transformed with plasmid pGA1903-U (lanes 7 to 11) or pGA1905 (lanes 12 and 13) were treated with α-factor at 0.1 μM, and samples were removed at the times (in minutes) indicated. Cell extracts were prepared, Fus3p-myc was immunoprecipitated with 1.7 μg of Myc1-9E10 antibody, and immune complex kinase assays were performed with 7.5 μg of myelin basic protein. (B) Parallel immunoprecipitations were performed with the extracts described for panel A, and a Western blot was prepared from these samples and probed with anti-myc antibody. (C) Strains and α-factor treatment were as described for panel A except that the time of sample removal is indicated in hours. (D) Parallel immunoprecipitations were performed with the extracts described for panel C, and a Western blot was prepared from these samples and probed with anti-myc antibody. (E) The fold induction of Fus3p kinase activity from the experiment shown in panel C was calculated as follows. Relative amounts of phosphate incorporated into MBP were determined by PhosphorImager analysis. After subtracting the amount incorporated by a sample that did not contain Fus3p-myc from all the other amounts, the fold induction was calculated as the amount incorporated at a given time point divided by the amount at the zero time point. Values obtained from *STE3*^{DAF} strains are shown in open squares, and values from *STE3* strains are shown in closed squares.

could be an indirect effect of reducing the amount of signal transmitted from an upstream step in the pathway.

Induction of Fus3p kinase activity is reduced at late times in *STE3*^{DAF} cells. Because *STE3*^{DAF} cells did not maintain Far1p phosphorylation, it was of interest to determine whether this effect involves inactivation of the Fus3p MAP kinase, which is thought to phosphorylate Far1p. To investigate the kinetics of activation of the signaling pathway, an immune complex kinase assay with myc-tagged Fus3p was performed (15). Extracts were prepared from *STE3* and *STE3*^{DAF} cells treated for various amounts of time with α-factor, and myc-tagged Fus3p was immunoprecipitated by using the anti-myc monoclonal antibody 9E10. The immunoprecipitates were incubated in kinase buffer with ^{32}P-labeled ATP and the MAP kinase substrate myelin basic protein (MBP), and the products of the reaction were separated by SDS-PAGE. *STE3* and *STE3*^{DAF} cells displayed a similar increase in Fus3p activity after 15 to 60 min of α-factor treatment (Fig. 3A, lanes 3 to 5 and 8 to 10). However, after 2 h of α-factor treatment, Fus3p activity in wild-type cells was higher than in *STE3*^{DAF} cells (Fig. 3A, lanes 6 and 11). Approximately equal amounts of Fus3p were shown to be present in each sample by probing a Western blot (immunoblot) of parallel immunoprecipitates with the anti-myc antibody (Fig. 3B). To demonstrate that the increase in phosphorylation of MBP in this assay was produced by a Fus3p-dependent activity, the assay was performed with the inactive Fus3p-K42R protein (18). The same background level of phosphorylated MBP was seen with extracts containing Fus3p-K42R as was seen with extracts that did not contain myc-tagged Fus3p (Fig. 3A, lanes 1, 12, and 13).

A longer time course experiment was performed to pursue the observation that Fus3p activity differed between wild-type and *STE3*^{DAF} cells treated with α-factor for more than 1 h. Whereas Fus3p from *STE3* cells displayed a high level of activity at all time points from 1 to 4 h (Fig. 3C, lanes 8 to 11), Fus3p from *STE3*^{DAF} cells displayed a peak of activity at 1 h that gradually declined at later time points (Fig. 3C, lanes 3 to 6). The results from Fig. 3C were quantified by PhosphorImager analysis, and a plot of the fold induction of Fus3p activity against duration of α-factor treatment is shown in Fig. 3E. The curves diverge at 2 h, when Fus3p activity slightly increased in wild-type cells and decreased in *STE3*^{DAF} cells. Analysis of data from several experiments showed that Fus3p activity from *STE3* and *STE3*^{DAF} cells was not significantly different at time points up to 1 h after pheromone treatment. At 2 h, however, induction of Fus3p activity from *STE3*^{DAF} cells was 3.1 ± 0.5, compared to 8.7 ± 1.2 (n = 3) for Fus3p from *STE3* cells.

***FUS1* transcript levels are reduced at late times in *STE3*^{DAF} cells but remain high in cycling *STE3* cells.** MAP kinase activation is known to be responsible for mediating cell cycle arrest and transcriptional activation of pheromone-inducible genes. A prediction of the results presented above is that transcrip-

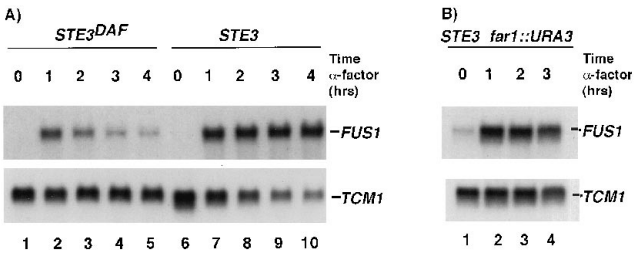

FIG. 4. *FUS1* transcript levels are decreased at late times after pheromone treatment of $STE3^{DAF}$ cells and remain high in cycling *STE3* cells. (A) $STE3^{DAF}$ (H67-6C.Ba) and *STE3* (H67-9D.Ba) strains were treated with α-factor at 0.1 μM for the indicated periods of time. RNA was isolated, transferred to nitrocellulose, and hybridized with *FUS1* probe. The blot was rehybridized with *TCM1* probe to determine the amount of RNA per lane. (B) A *STE3 far1::URA3* strain (AC12) was treated with 0.1 μM α-factor for the indicated periods of time. RNA extraction and Northern blot analysis were performed as for panel A.

tional induction would also lack sustained activation in a $STE3^{DAF}$ strain. To test this idea, RNA was prepared from wild-type and $STE3^{DAF}$ cells at different time points after addition of α-factor to observe changes in the expression of *FUS1*. As expected, wild-type cells exhibited an increase in *FUS1* RNA levels after 1 h of treatment with pheromone (Fig. 4A, lanes 6 and 7), and the induction remained high for at least 4 h (Fig. 4A, lanes 7 to 10). In contrast, *FUS1* RNA levels in $STE3^{DAF}$ cells increased during the first hour and then decreased gradually (Fig. 4A, lanes 1 to 5), closely resembling the kinetics of Fus3p inactivation. Because $STE3^{DAF}$ cells continue to cycle after pheromone treatment, one interpretation of these results is that the decrease in *FUS1* RNA seen under these conditions is a consequence of cell cycle progression. To test this idea, a time course of *FUS1* RNA induction was performed with *STE3* cells that contain a Δ*far1* mutation, which confers a specific defect in cell cycle arrest. *STE3* Δ*far1* cells displayed high levels of *FUS1* RNA for 3 h after pheromone treatment while the cells were actively cycling (Fig. 4B, lanes 2 to 4). This finding demonstrates that progression of the cell cycle does not affect transcriptional induction.

In summary, the results presented thus far show that receptor inhibition causes a loss of activity of the signaling cascade at late times after pheromone treatment and that this phenomenon is reflected in the major events that occur in response to pheromone.

The $STE3^{DAF}$ effect cannot be mimicked with low doses of pheromone. One interpretation of the $STE3^{DAF}$ phenotype is that cell cycle arrest requires sustained signaling and that the presence of the **a**-factor receptor somehow decreases the total amount of signal. This situation might generate a transient activation of the pathway. If this were the case, it should be possible to reproduce the $STE3^{DAF}$ phenotype by treating cells with very low doses of pheromone. To test this possibility, wild-type cells were treated with α-factor at 10-fold dilutions from 10^{-7} to 10^{-10} M. RNA was prepared after 1 and 3 h of α-factor addition, and the percentage of unbudded cells was determined at 3 h. Treatment of cells with α-factor at 10^{-7} M caused complete arrest and a high level of *FUS1* RNA induction at 1 and 3 h (Fig. 5, lanes 1 and 2). Cells treated with 10^{-8} M α-factor displayed an induced level of *FUS1* RNA that was about 50% of the full level but showed nearly complete cell cycle arrest (Fig. 5, lanes 3 and 4). In contrast, $STE3^{DAF}$ cells treated with 10^{-7} M α-factor displayed nearly full transcriptional induction at 1 h of pheromone treatment (Fig. 4A, lanes 2 and 7) but showed no cell cycle arrest (percentage of unbudded cells was 55 ± 1 with α-factor and 53 ± 2 without α-factor). Moreover, wild-type cells treated with concentrations of pheromone that did not induce cell cycle arrest did not display either a prolonged or a transient increase in *FUS1* transcriptional levels (Fig. 5, lanes 5 to 8). These data indicate that the $STE3^{DAF}$ phenotype cannot be mimicked by low doses of pheromone and, thus, that the observed inactivation of the signaling cascade is not due to an overall decrease in the level of signal.

$STE3^{DAF}$* acts between *STE4* and *STE5*.** Ordering of the steps in the pheromone response pathway has been accomplished by double mutant analysis, in which cells containing both a constitutive mutation and a signaling-defective mutation have been assayed for a response. To analyze the step at which receptor inhibition acts, $STE3^{DAF}$ and control strains were transformed with plasmids carrying inducible genes that cause constitutive activation of the pathway. The *STE4* gene, which encodes the G_β subunit, has been shown to cause cells to arrest when it is overexpressed from the *GAL* promoter (5, 39, 52). As expected, overexpression of *STE4* in wild-type *MATa** cells caused growth arrest (Fig. 6A). *STE4* overexpression had no effect in wild-type diploid cells or haploid *ste12*::*LEU2* cells (6), demonstrating that *STE4*-dependent growth arrest is mediated by the pheromone response pathway. However, the $STE3^{DAF}$ allele prevented the arrest phenotype conferred by overexpression of *STE4*. This finding agrees with the previous observation that $STE3^{DAF}$ can suppress the constitutive $STE4^{Hpl}$ allele (26) and suggests that $STE3^{DAF}$ acts at or downstream of *STE4*.

The pheromone response pathway impinges on two MAP kinases, Fus3p and Kss1p, which are partially redundant for function. Strains containing null alleles of both genes are completely sterile and cannot activate the pheromone signaling pathway. However, individual Δ*fus3* or Δ*kss1* strains are capable of responding to pheromone, although Δ*fus3* strains arrest only at high doses of pheromone. Assays performed on these strains showed that the $STE3^{DAF}$ allele eliminated the large, clear halo produced by a Δ*kss1* strain, as well as the small, filled-in halo produced by a Δ*fus3* strain (6). Inhibition of cell cycle arrest by $STE3^{DAF}$ in strains lacking either one or the other of the MAP kinases is consistent with the idea that $STE3^{DAF}$ acts upstream of MAP kinase activation. To determine if receptor inhibition acts on an upstream step, the

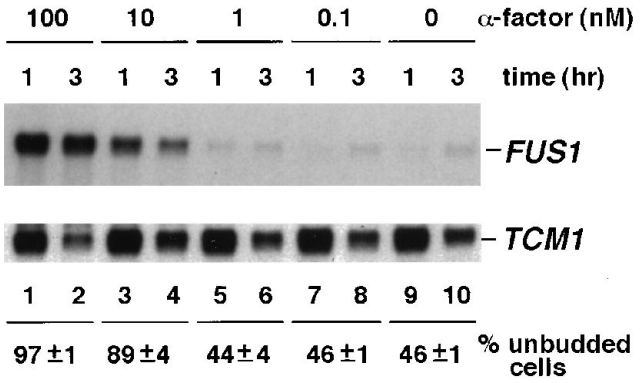

FIG. 5. The $STE3^{DAF}$ effect cannot be mimicked with low doses of pheromone. A *STE3* strain (H67-9D.Ba) was treated with α-factor at the indicated concentrations for 1 and 3 h, and RNA was isolated. Northern blots were prepared as described in the legend to Fig. 4. The percentage of unbudded cells was calculated by counting the number of budded cells in a total of 200 cells after 3 h of treatment with α-factor at 0.1 μM. The counting process was repeated three times and an average of the individual counts was calculated and converted to percent unbudded.

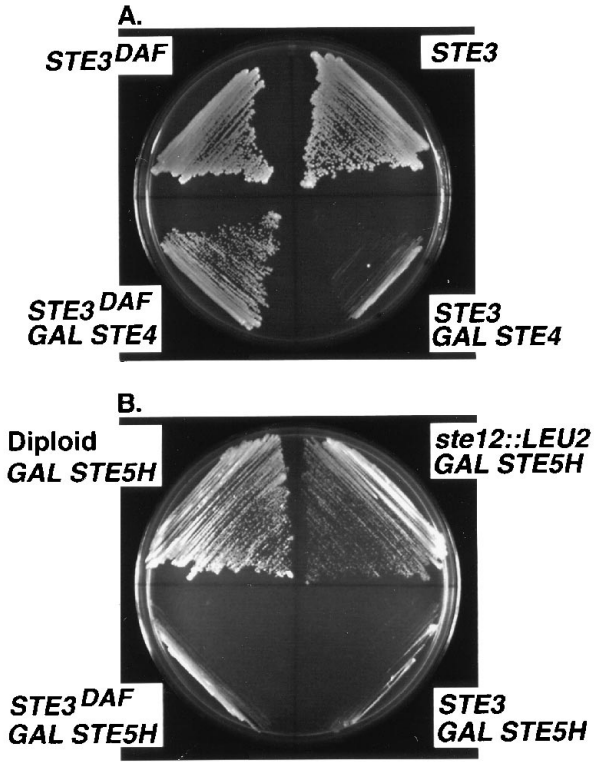

FIG. 6. $STE3^{DAF}$ acts between *STE4* and *STE5*. (A) $STE3^{DAF}$ (H67-6C.Ba) and *STE3* (H67-9D.Ba) strains were transformed either with a plasmid containing *STE4* under the control of the *GAL* promoter (pL19) (52) or with vector alone (pBM272). Cells were streaked onto galactose-containing plates and grown at 30°C for 2 to 3 days. (B) The strains described for panel A were transformed with a plasmid containing $STE5^{Hyp}$ under the control of the *GAL* promoter (pGAL-STE5H). Control wild-type diploid (W303) and haploid *ste12*::*LEU2* (D109-1B) strains were also transformed with pGAL-STE5H. Cells were streaked onto galactose-containing plates and grown at 30°C for 2 to 3 days.

$STE3^{DAF}$ allele was tested for its ability to suppress the arrest phenotype conferred by a hyperactive allele of *STE5* (21), which encodes a scaffolding protein that assembles the MAP kinase cascade into a complex (4, 42). Overexpression of the $STE5^{Hyp}$ allele caused cell cycle arrest in both *STE3* and $STE3^{DAF}$ cells (Fig. 6B), suggesting that $STE3^{DAF}$ acts at or upstream of *STE5*. $STE5^{Hyp}$ overexpression had no effect in wild-type diploid cells or haploid *ste12*::*LEU2* cells (Fig. 6B), demonstrating that the effect of this allele depends on the pheromone response pathway.

Overexpression of *STE20* blocks the $STE3^{DAF}$ effect. One component of the signaling pathway that acts downstream of G protein subunit dissociation and upstream of the MAP kinase cascade is the Ste20p protein kinase (29, 44). To determine if Ste20p is involved in receptor inhibition, the effect of *STE20* overexpression on the $STE3^{DAF}$ phenotype was tested. In the absence of α-factor, overexpression of full-length *STE20* in either *STE3* or $STE3^{DAF}$ cells did not cause cell cycle arrest (Fig. 7, top), indicating that increased levels of wild-type Ste20p do not activate the pathway. In the presence of α-factor, overexpression of *STE20* suppressed the $STE3^{DAF}$ phenotype, resulting in pheromone-induced arrest of the $STE3^{DAF}$ strain (Fig. 7, bottom). Although other explanations can account for this result, one interpretation of the finding that *STE20* overexpression bypasses the effect of $STE3^{DAF}$ is that the receptor acts at a step that is subject to direct competition by excess Ste20p.

DISCUSSION

Receptor inhibition occurs when a pheromone receptor expressed in the inappropriate haploid cell type blocks the cell cycle arrest response to pheromone. Here we show that this effect consists of a late inactivation of the signaling pathway that allows the cells to escape arrest. Investigation of this phenomenon allowed us to determine that sustained MAP kinase activation is associated with cell cycle arrest, whereas transient activation is sufficient for early transcriptional induction. We have also shown that the site of receptor-mediated inhibition is limited to a subset of signaling events. Inhibition must occur downstream of G protein subunit dissociation because the receptor inhibitory function blocks the constitutive arrest phenotype of cells lacking the G_α subunit (26) or overexpressing the G_β subunit. It is also limited to an event at or upstream of the Ste5p step, because it does not inhibit activation of the pathway by a constitutive *STE5* mutation. Ste5p appears to function as a scaffold for the assembly of proteins that comprise the MAP kinase cascade. Therefore, it is likely that receptor inhibition acts upstream of the initiation of this phosphorylation cascade. Moreover, receptor inhibition is substantially blocked by overexpression of *STE20*, a finding that is consistent with the idea that excess Ste20p overcomes an inhibitory interaction mediated by the receptor. Recent evidence suggests that activation of the pheromone response pathway requires stimulation of Ste20p kinase activity by the Rho-type GTPase Cdc42p (48, 54). Activation of Cdc42p may occur through the binding of its guanine nucleotide exchange factor,

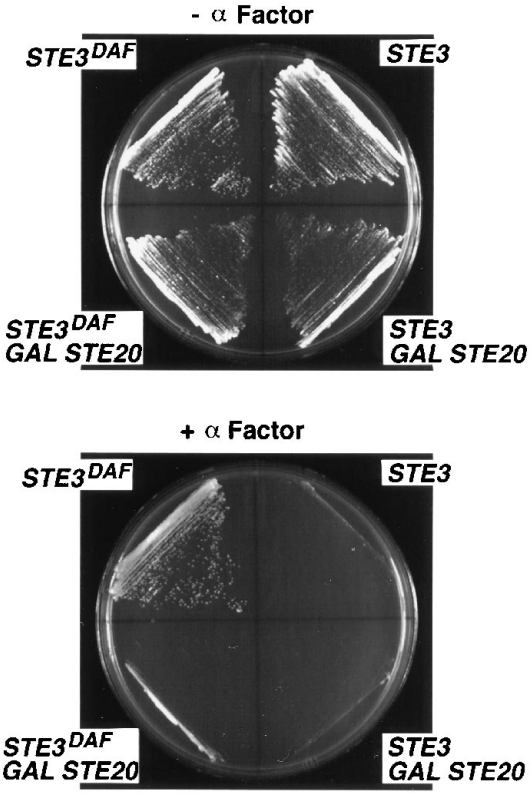

FIG. 7. Overexpression of *STE20* blocks the $STE3^{DAF}$ effect. $STE3^{DAF}$ (H67-6C.Ba) and *STE3* (H67-9D.Ba) strains were transformed either with a plasmid containing *STE20* under the control of the *GAL* promoter (pMSTE20-L2) or with vector alone (pRS315). Cells were streaked on a galactose-containing plate either without (top panel) or with (bottom panel) 20 μl of 1 mM α-factor.

Cdc24p, to the G protein β subunit (54). Because Cdc42p is known to be present at the plasma membrane within mating projections (56), it seems likely that Cdc24p, Cdc42p, and Ste20p are all localized in close proximity to the pheromone receptors. This signaling module is therefore positioned such that it could be directly bound and inhibited by inappropriately expressed receptor.

A striking parallel exists between the profile of the pheromone response during receptor inhibition and the differential responses of the PC12 pheochromocytoma cell line to extracellular growth and differentiation factors. Treatment of PC12 cells with nerve growth factor (NGF) causes them to undergo cell cycle arrest and differentiate into sympathetic neuron-like cells, whereas treatment with epidermal growth factor (EGF) causes them to proliferate (34). The NGF and EGF receptors are tyrosine kinases that activate a *ras*-dependent signal transduction pathway and result in activation of MAP kinases. NGF stimulation causes an increase in MAP kinase activity that persists for several hours, while EGF stimulation produces an equal initial burst of MAP kinase activity that decreases to near basal level by 1 h (19, 23, 43, 50). Stimulation of PC12 cells by the physiologically relevant factor NGF thus parallels stimulation of wild-type yeast cells with pheromone, which caused an increase in Fus3p MAP kinase activity that persisted for up to 4 h. Both systems respond to sustained activation of MAP kinase activity by cell cycle arrest and alteration of cellular morphology. In the case of EGF stimulation of PC12 cells, transient MAP kinase activation results in cell division without the changes in morphology that accompany differentiation. The onset of cell division probably involves transcriptional induction of early genes involved in proliferation (25). Likewise, pheromone stimulation of cells expressing an inappropriate receptor caused a transient activation of MAP kinase which produced a transient transcriptional induction response with only minor changes in morphology (6). One differential effect of the duration of MAP kinase activation in PC12 cells is that only sustained activation results in nuclear translocation of MAP kinase (38, 50). The subcellular distribution of the yeast Fus3p MAP kinase has not been investigated, although the location of Kss1p is predominantly nuclear and does not appear to change after activation of the signaling pathway (33). Therefore, the downstream events that result in cell cycle arrest probably take place in the nucleus in both the mammalian and yeast systems.

Uncoupling of cell cycle arrest and transcriptional induction is a phenotype that has been seen for mutations in other genes that encode signaling proteins. For example, the functions of the Fus3p and Kss1p MAP kinases are partially overlapping, but deletion of the *FUS3* gene substantially eliminates cell cycle arrest without affecting transcriptional induction (12, 51). On the basis of our results, one interpretation of this observation could be that activation of Kss1p is short-lived. Alternatively, it is possible that Kss1p can supply the transcriptional induction function but not the cell cycle arrest function of Fus3p. Likewise, dominant alleles of *STE4* have been isolated that affect arrest more than transcriptional induction and that appear to act on a late phase of the response (20, 30). We have investigated the duration of the pheromone response under these conditions and have found that transcriptional induction is sustained for several hours both in Δ*fus3* cells and in cells expressing the dominant *STE4-D62N* mutation (6). Therefore, the transient activation of the pheromone response seen under conditions of receptor inhibition is a unique process that does not occur under other circumstances in which cells continue to cycle in the presence of pheromone. This process may have evolved to ensure that cell division continues during times when cells express a receptor that is inappropriate to their *MAT* allele. Such times in the yeast life cycle include the period after mating type switching and the period following zygote formation. Receptor inhibition could function to prevent arrest of the cell cycle in cells undergoing these processes.

Several different models for the action of receptor inhibition can be proposed to explain our results. First, inappropriate expression of pheromone receptor could cause the activation of a desensitization process that normally occurs later during the response. Unlike most aspects of desensitization that have been studied (49), this process would be expected to exert its effect downstream of the G protein. It would also be expected to be independent of *SST2*, a gene that is not involved in signaling but appears to have a desensitization function (1, 10), because the $STE3^{DAF}$ allele blocks cell cycle arrest in an *sst2* mutant strain (26). Alternatively, inappropriately expressed receptor could allow the initial stages of signaling to take place but could interfere with amplification of the signal through a positive feedback loop. Such a positive feedback loop involving Cdc28p/Cln activity is thought to control the expression of the *CLN1* and *CLN2* genes during G_1 (8, 11). Several kinases in the pheromone response pathway phosphorylate upstream signaling components, and the consequences of these modifications are unknown, so the potential for a feedback loop exists in this signaling pathway (28, 55). Finally, it is possible that pheromone binding activates more than one signal transduction pathway that acts on the Fus3p MAP kinase and that inappropriate expression of receptor blocks an alternative pathway to MAP kinase activation. Several MAP kinase cascades exist in *S. cerevisiae* (24), and the potential exists for cross talk among the pathways. Further experiments will be necessary to distinguish between these models for the action of the $STE3^{DAF}$ allele.

ACKNOWLEDGMENTS

We thank G. Ammerer, B. Cairns, W. Courchesne, F. Cross and J. McKinney, E. Elion, B. Errede, B. Futcher, D. Jenness, S. Michaelis, and M. Whiteway for providing plasmids used in this work; F. Cross and J. McKinney for the gift of anti-Far1p antisera; and B. Errede and B. Buehrer for advice on the immune complex kinase assay.

This work was supported by National Institutes of Health grant GM48808.

REFERENCES

1. **Chan, R. K., and C. A. Otte.** 1982. Isolation and genetic analysis of *Saccharomyces cerevisiae* mutants supersensitive to G1 arrest by **a** factor and α factor pheromones. Mol. Cell. Biol. **2:**11–20.
2. **Chang, F., and I. Herskowitz.** 1990. Identification of a gene necessary for cell cycle arrest by a negative growth factor of yeast: FAR1 is an inhibitor of a G1 cyclin, CLN2. Cell **63:**999–1011.
3. **Chang, F., and I. Herskowitz.** 1992. Phosphorylation of FAR1 in response to α-factor: a possible requirement for cell-cycle arrest. Mol. Biol. Cell **3:**445–450.
4. **Choi, K. Y., B. Satterberg, D. M. Lyons, and E. A. Elion.** 1994. Ste5 tethers multiple protein kinases in the MAP kinase cascade required for mating in S. cerevisiae. Cell **78:**499–512.
5. **Cole, G. M., D. E. Stone, and S. I. Reed.** 1990. Stoichiometry of G protein subunits affects the *Saccharomyces cerevisiae* mating pheromone signal transduction pathway. Mol. Cell. Biol. **10:**510–517.
6. **Couve, A., and J. P. Hirsch.** Unpublished data.
7. **Cross, F. R.** 1990. The *DAF2-2* mutation, a dominant inhibitor of the *STE4* step in the α-factor signalling pathway of *Saccharomyces cerevisiae MAT***a** cells. Genetics **126:**301–308.
8. **Cross, F. R., and A. H. Tinkelenberg.** 1991. A potential positive feedback loop controlling *CLN1* and *CLN2* gene expression at the start of the yeast cell cycle. Cell **65:**875–883.
9. **Daugherty, B. L., J. A. DeMartin, M. F. Law, D. W. Kawka, and M. G. E. Singer II.** 1991. Polymerase chain reaction facilitates the cloning, CDR-grafting, and rapid expression of a murine monoclonal antibody directed against the CD18 component of leukocyte integrins. Nucleic Acids Res. **19:**2471–2476.

10. **Dietzel, C., and J. Kurjan.** 1987. Pheromonal regulation and sequence of the *Saccharomyces cerevisiae SST2* gene: a model for desensitization to pheromone. Mol. Cell. Biol. **7:**4169–4177.
11. **Dirick, L., and K. Nasmyth.** 1991. Positive feedback in the activation of G1 cyclins in yeast. Nature (London) **351:**754–757.
12. **Elion, E. A., J. A. Brill, and G. R. Fink.** 1991. *FUS3* represses *CLN1* and *CLN2* and in concert with *KSS1* promotes signal transduction. Proc. Natl. Acad. Sci. USA **88:**9392–9396.
13. **Elion, E. A., B. Satterberg, and J. E. Kranz.** 1993. FUS3 phosphorylates multiple components of the mating signal transduction cascade: evidence for STE12 and FAR1. Mol. Biol. Cell **4:**495–510.
14. **Errede, B., and G. Ammerer.** 1989. STE12, a protein involved in cell-type-specific transcription and signal transduction in yeast, is part of protein-DNA complexes. Genes Dev. **3:**1349–1361.
15. **Errede, B., A. Gartner, Z. Zhou, K. Nasmyth, and G. Ammerer.** 1993. MAP kinase-related FUS3 from *S. cerevisiae* is activated by STE7 *in vitro*. Nature (London) **362:**261–264.
16. **Errede, B., and D. E. Levin.** 1993. A conserved kinase cascade for MAP kinase activation in yeast. Curr. Opin. Cell Biol. **5:**254–260.
17. **Evan, G. I., G. K. Lewis, G. Ramsay, and J. M. Bishop.** 1985. Isolation of monoclonal antibodies specific for human c-*myc* proto-oncogene product. Mol. Cell. Biol. **5:**3610–3616.
18. **Gartner, A., K. Nasmyth, and G. Ammerer.** 1992. Signal transduction in *Saccharomyces cerevisiae* requires tyrosine and threonine phosphorylation of FUS3 and KSS1. Genes Dev. **6:**1280–1292.
19. **Gotoh, Y., E. Nishida, T. Yamashita, M. Hoshi, M. Kawakami, and H. Sakai.** 1990. Microtubule-associated-protein (MAP) kinase activated by nerve growth factor and epidermal growth factor in PC12 cells. Eur. J. Biochem. **193:**661–669.
20. **Grishin, A. V., J. L. Weiner, and K. J. Blumer.** 1994. Control of adaptation to mating pheromone by G protein β subunits of *Saccharomyces cerevisiae*. Genetics **138:**1081–1092.
21. **Hasson, M. S., D. Blinder, J. Thorner, and D. D. Jenness.** 1994. Mutational activation of the *STE5* gene product bypasses the requirement for G protein β and γ subunits in the yeast pheromone response pathway. Mol. Cell. Biol. **14:**1054–1065.
22. **Hausdorff, W. P., M. G. Caron, and R. J. Lefkowitz.** 1990. Turning off the signal: desensitization of β-adrenergic receptor function. FASEB J. **4:**2881–2889.
23. **Heasley, L. E., and G. L. Johnson.** 1992. The β-PDGF receptor induces neuronal differentiation of PC12 cells. Mol. Biol. Cell **3:**545–553.
24. **Herskowitz, I.** 1995. MAP kinase pathways in yeast: for mating and more. Cell **80:**187–197.
25. **Hill, C. S., and R. Treisman.** 1995. Transcriptional regulation by extracellular signals: mechanisms and specificity. Cell **80:**199–211.
26. **Hirsch, J. P., and F. R. Cross.** 1993. The pheromone receptors inhibit the pheromone response pathway in *Saccharomyces cerevisiae* by a process that is independent of their associated Gα protein. Genetics **135:**943–953.
27. **Ito, H., Y. Fukuda, K. Murata, and A. Kimura.** 1983. Transformation of intact yeast cells with alkali cations. J. Bacteriol. **153:**163–168.
28. **Kranz, J. E., B. Satterberg, and E. A. Elion.** 1994. The MAP kinase Fus3 associates with and phosphorylates the upstream signaling component Ste5. Genes Dev. **8:**313–327.
29. **Leberer, E., D. Dignard, D. Harcus, D. Y. Thomas, and M. Whiteway.** 1992. The protein kinase homologue Ste20p is required to link the yeast pheromone response G-protein βγ subunits to downstream signalling components. EMBO J. **11:**4815–4824.
30. **Leberer, E., D. Dignard, L. Hougan, D. Y. Thomas, and M. Whiteway.** 1992. Dominant-negative mutants of a yeast G-protein β subunit identify two functional regions involved in pheromone signalling. EMBO J. **11:**4805–4813.
31. **Lefkowitz, R. J.** 1993. G protein-coupled receptor kinases. Cell **74:**409–412.
32. **Lehrach, H., D. Diamond, J. M. Wozney, and H. Boedtker.** 1977. RNA molecular weight determinations by gel electrophoresis under denaturing conditions, a critical reexamination. Biochemistry **16:**4743–4751.
33. **Ma, D., J. G. Cook, and J. Thorner.** 1995. Phosphorylation and localization of Kss1, a MAP kinase of the *Saccharomyces cerevisiae* pheromone response pathway. Mol. Biol. Cell **6:**889–909.
34. **Marshall, C. J.** 1995. Specificity of receptor tyrosine kinase signaling: transient versus sustained extracellular signal-regulated kinase activation. Cell **80:**179–185.
35. **McCaffrey, G., F. J. Clay, K. Kelsay, and G. F. Sprague, Jr.** 1987. Identification and regulation of a gene required for cell fusion during mating of the yeast *Saccharomyces cerevisiae*. Mol. Cell. Biol. **7:**2680–2690.
36. **McKinney, J. D., and F. R. Cross.** 1995. *FAR1* and the G_1 phase specificity of cell cycle arrest by mating factor in *Saccharomyces cerevisiae*. Mol. Cell. Biol. **15:**2509–2516.
37. **Michaelis, S., and I. Herskowitz.** 1988. The **a**-factor pheromone of *Saccharomyces cerevisiae* is essential for mating. Mol. Cell. Biol. **8:**1309–1318.
38. **Nguyen, T. T., J. Scimeca, C. Filloux, P. Peraldi, J. Carpentier, and E. Van Obberghen.** 1993. Co-regulation of the mitogen-activated protein kinase, extracellular signal-regulated kinase 1, and the 90-kDa ribosomal S6 kinase in PC12 cells. J. Biol. Chem. **268:**9803–9810.
39. **Nomoto, S., N. Nakayama, K. Arai, and K. Matsumoto.** 1990. Regulation of the yeast pheromone response pathway by G protein subunits. EMBO J. **9:**691–696.
40. **Peter, M., A. Gartner, J. Horecka, G. Ammerer, and I. Herskowitz.** 1993. FAR1 links the signal transduction pathway to the cell cycle machinery in yeast. Cell **73:**747–760.
41. **Peter, M., and I. Herskowitz.** 1994. Direct inhibition of the yeast cyclin-dependent kinase Cdc28-Cln by Far1. Science **265:**1228–1231.
42. **Printen, J. A., and G. F. Sprague, Jr.** 1994. Protein-protein interactions in the yeast pheromone response pathway: Ste5p interacts with all members of the MAP kinase cascade. Genetics **138:**609–619.
43. **Qiu, M., and S. H. Green.** 1992. PC12 cell neuronal differentiation is associated with prolonged $p21^{ras}$ activity and consequent prolonged ERK activity. Neuron **9:**705–717.
44. **Ramer, S. W., and R. W. Davis.** 1993. A dominant truncation allele identifies a gene, *STE20*, that encodes a putative protein kinase necessary for mating in *Saccharomyces cerevisiae*. Proc. Natl. Acad. Sci. USA **90:**452–456.
45. **Schultz, L. D., and J. D. Friesen.** 1983. Nucleotide sequence of the *tcm1* gene (ribosomal protein L3) of *Saccharomyces cerevisiae*. J. Bacteriol. **155:**8–14.
46. **Sherman, F., G. R. Fink, and J. B. Hicks.** 1989. Laboratory course manual for methods in yeast genetics. Cold Spring Harbor Laboratory, Plainview, N.Y.
47. **Sikorski, R. S., and P. Hieter.** 1989. A system of shuttle vectors and yeast host strains designed for efficient manipulation of DNA in *Saccharomyces cerevisiae*. Genetics **122:**19–27.
48. **Simon, M., C. De Virgilio, B. Souza, J. R. Pringle, A. Abo, and S. I. Reed.** 1995. Role for the Rho-family GTPase Cdc42 in yeast mating-pheromone signal pathway. Nature (London) **376:**702–705.
49. **Sprague, G. F., Jr., and J. W. Thorner.** 1992. Pheromone response and signal transduction during the mating process of *Saccharomyces cerevisiae*, p. 657–744. *In* E. W. Jones, J. R. Pringle, and J. R. Broach (ed.), The Molecular and cellular biology of the yeast Saccharomyces: gene expression. Cold Spring Harbor Laboratory Press, Plainview, N.Y.
50. **Traverse, S., N. Gomez, H. Paterson, C. Marshall, and P. Cohen.** 1992. Sustained activation of the mitogen-activated protein (MAP) kinase cascade may be required for differentiation of PC12 cells. Biochem. J. **288:**351–355.
51. **Tyers, M., and B. Futcher.** 1993. Far1 and Fus3 link the mating pheromone signal transduction pathway to three G_1-phase Cdc28 kinase complexes. Mol. Cell. Biol. **13:**5659–5669.
52. **Whiteway, M., L. Hougan, and D. Y. Thomas.** 1990. Overexpression of the STE4 gene leads to mating response in haploid *Saccharomyces cerevisiae*. Mol. Cell. Biol. **10:**217–222.
53. **Yuan, Y. O., and S. Fields.** 1991. Properties of the DNA-binding domain of the *Saccharomyces cerevisiae* STE12 protein. Mol. Cell. Biol. **11:**5910–5918.
54. **Zhao, Z., T. Leung, E. Manser, and L. Lim.** 1995. Pheromone signalling in *Saccharomyces cerevisiae* requires the small GTP-binding protein Cdc42p and its activator CDC24. Mol. Cell. Biol. **15:**5246–5257.
55. **Zhou, Z., A. Gartner, R. Cade, G. Ammerer, and B. Errede.** 1993. Pheromone-induced signal transduction in *Saccharomyces cerevisiae* requires the sequential function of three protein kinases. Mol. Cell. Biol. **13:**2069–2080.
56. **Ziman, M., D. Preuss, J. Mulholland, J. M. O'Brien, D. Botstein, and D. I. Johnson.** 1993. Subcellular localization of Cdc42p, a *Saccharomyces cerevisiae* GTP-binding protein involved in the control of cell polarity. Mol. Biol. Cell **4:**1307–1316.